

# TWO PHASE FLOWS IMAGING BY ELECTRICAL IMPEDANCE TOMOGRAPHY: PRELIMINARY STUDIES TO IMPROVE AN OPTIMIZATION BASED RECONSTRUCTION TECHNIQUE

**G.L.C. Carosio**

**V. P. Rolnik**

**P. Seleghim Jr.**

Núcleo de Engenharia Térmica e Fluidos  
Escola de Engenharia de São Carlos  
Universidade de São Paulo  
Av. Trabalhador São-carlense, 400  
13566-590 São Carlos – SP – Brazil  
seleghim@sc.usp.br

**Abstract.** *The main objective of this work is to contribute to the development of a new two-phase flow tomographic reconstruction method suited for processing signals obtained from electrical or other soft field sensing probes. Electrical impedance tomography (EIT) is an inexpensive and sufficiently robust sensing technique, perfectly applicable to industrial process. Generally, the approach consists in devising an error functional that confront two different models of the same problem with the same excitation profile: one implemented on a digital computer through a numerical discretization of the governing equation and the other analogically implemented on the experimental setup. The error surface is constructed numerically by establishing the actual phase distribution and changing the approximated one and, generally, it presents characteristics on its topology, which we call pathologies. Some pathologies detected until now reveal the existence of saddle points, boundary minima and nearly flat region surrounding the solution well, which may seriously compromise the effectiveness of numerical minimization method. Nevertheless, both the form of the error functional and the excitation profile influence the topology of the error surface and, consequently, the success of the minimization method. An extensive preliminary study about different errors functional and improved excitation profiles is mandatory to guarantee a good convergence for the optimization method. Numerical simulations have been performed aiming to demonstrate the feasibility of our approach. The sensing volume was a 1:1:3 non-dimensional parallelepiped with different voltage profiles imposed on its longitudinal boundaries (excitation) and no-flux condition imposed on the transversal boundaries. The flowing two-phase mixture corresponds to distilled water ( $S = 80$ ) with a small three-dimensional air inclusion ( $S = 1$ ).*

**Keywords.** *Process tomography, reconstruction method, optimization, multiphase flow*

## 1. Introduction

Electrical impedance measurements (resistive, capacitive and inductivity) constitute one of the most appropriated sensing technique for industrial processes, mainly due to their low cost of installation, simple utilization and maintenance, robustness and applicability in non-controlled environments. Electrical impedance tomography (EIT) is an inverse problem which consists on determining the electric contrast distribution in the interior of a sensing volume by applying an excitation profile on the external surface and measuring the corresponding response on the same surface. The data obtained this way is supplied to a computer with a specific software that reconstruct the original image. The approach used in this paper to perform the tomographic reconstruction of phase distribution in two-phase flows consists on minimizing an error functional that expresses the difference between actual measurements, experimentally obtained, and the approximated measurements obtained numerically from an approximated contrast distribution. The global minimum of the error functional corresponds to the sought image, provided that some technical conditions are satisfied to assure existence and uniqueness of the solution of the EIT problem. Despite the simplicity of this stimulus-and-response approach, the problem is intrinsically ill-posed and, consequently, questions about the stability of the solution in the presence of experimental errors are complex and, in fact, are still being studied. Existence and uniqueness are proved by Nachman (1988), although his reconstruction algorithm is unstable in practice due to exponential amplification of noise and is not applicable in high contrast flows.

The main consequence of instability (or ill-conditioning) is the extreme sensitivity of the solution in the presence of errors, including experimental errors in the data and truncation errors in the computational procedure. In addition, it is a well known fact that current reconstruction techniques are inadequate, that is, have poor resolution, low distinguishability and, often, produce spurious artifacts (void fractions lower than 0 or higher than 1 for example – Lanvy, 1998) which need to be corrected a posteriori. These reasons probably explain why tomographic techniques are not intensively applied in industrial processes, despite the great insight and optimization possibilities that it may bring.

Geometric features such as extremely pronounced global minimum (the solution well), multiple minima, saddle points, boundary minima and flat regions constitute a set of common characteristics, called pathology of the optimization surface (Rolnik and Seleghim, 2001, Campos *et al.*, 2002), and can be interpreted as the manifestation of the ill-conditioned nature of the inverse problem according to the adopted formulation. The pathologies may seriously compromise the effectiveness of numerical minimization methods. Regularizations schemes must be used to assure stability of the reconstruction procedure. Basically all the know regularization methods make use of some a priori information about the unknown property. However, few researchers are worried about the difficulties associated with practical implementation of the method, particularly in industrial two-phase flows tomography in which measurements tend to be more complex due to harsh environmental conditions. The formulation of the problem is so that the inclusion

of additional information that contributes to the reconstruction process can be done in a very straightforward manner. In addition to the external excitation and response measurements, the error functional can take into account additional physical measurements such as, for instance, the phase fraction.

This paper presents preliminary studies of regularization strategies that consist basically in introducing a priori information based on mathematical, computational and physic knowledge of the problem. With this purpose, an extensive study about the pathologies of the error function is performed considering different excitation profiles and different error functional formulas in order to show that different error functionals can present completely diferent properties and behaviour. These studies are crucial for the development of feasible reconstruction strategies, based on iteratively refining an initial guess image, which would be capable of reconstructing the correct electrical contrast distribution of the flowing two-phase mixture, from signals delivered by a direct imaging probe or any other soft field sensing device.

## 2. Statement of the problem

The governing non-dimensional equations of an electrical impedance tomography problem can be derived from Maxwell equations according to the following:

$$\bar{\nabla} \cdot (-\sigma \bar{\nabla} \phi) = 0 \quad \text{in } \Omega \quad (1)$$

$$\phi(\xi, \eta) = \phi_{\text{exc}}(\xi, \eta) \quad \text{for } (\xi, \eta) \in \partial \Omega \quad (2)$$

$$Q_{\text{meas}}(\xi, \eta) = -\sigma \bar{\nabla} \phi \Big|_{\xi, \eta} \quad \text{for } (\xi, \eta) \in \partial \Omega \quad (3)$$

where  $\phi$  represents the electric field,  $\sigma$  the medium's contrast (conductivity, permittivity or permeability),  $\phi_{\text{exc}}(\xi, \eta)$  the excitation profile and  $Q_{\text{meas}}(\xi, \eta)$  the measured profile (resulting electric currents or charge or profiles). The variables  $\phi_{\text{exc}}$  and  $Q_{\text{meas}}$  represent the relation between stimulus and response and shall be used to reconstruct the internal contrast  $\sigma$  within the sensing volume  $\Omega$ . Formally speaking, the response  $Q_{\text{meas}}$  is canonically conjugated to  $\phi_{\text{exc}}$  and  $\sigma$  through the formal operator (direct problem)

$$Q_{\text{meas}}(\xi, \eta) = \mathfrak{I}[\phi_{\text{exc}}, \sigma] \quad (4)$$

and the reconstruction problem can be interpreted as inverting  $\mathfrak{I}$  with respect to  $\sigma$ , that is (inverse problem)

$$\sigma = \mathfrak{I}^{-1}[\phi_{\text{exc}}, Q_{\text{meas}}] \quad (5)$$

There are many questions involving theoretical and practical issues associated to this problem. In particular, questions about existence, uniqueness and stability of solutions must be considered. For instance, the intensity and the way that small perturbations in the input or measured data influence the numerical reconstruction of the solution are still open questions. A good example of this can be found in the work developed by Seleglim and Milioli (2001) which quantify the sensitivity by studying the problem of reconstruction bubble size histograms from pierced length histograms in bubbly flow. Adopting a similar approach as the one adopted here they observed that relative errors of less than 0.001% in the input data could completely corrupt the calculations, producing astonishing deviations of more than 1000% in the reconstructed distributions. A theoretical framework for this problem was originally proposed by Hadamard (1902) who stated that the solution of a well-posed problem needs to satisfy simultaneously the three following conditions: a) existence, b) uniqueness and c) continuum and smooth dependence on the input data. In this sense, both Dirichlet boundary problem (Eqs. (1) and (2)) and Neumann boundary problem (Eqs. (1) and (3)) are well-posed (note that in the case of Neumann condition, all possible solutions are different by a constant). In other words, the direct problem consists thus in solving the differential equation (1) with one boundary condition (2) or (3) for a known medium's contrast  $\sigma$  and the internal electric field  $\phi_{\text{exc}}$  in the boundary.

In opposition to this,  $\sigma$  and  $\phi$  being unknown, equation (1) needs to be solved with both boundary conditions, that is, equations (2) and (3) simultaneously. In this case, the measured data  $Q_{\text{meas}}$  delivered by the probe is related to the medium's contrast  $\sigma$  through strongly ill-conditioned differential and/or integral operators, which explain the instability of the EIT problem. Nachman, 1998 proved the uniqueness to solution of the inverse problem for a  $C^{1,1}$  boundary and the contrast distribution  $\sigma$  in  $C^{1,1}$ . However, Hadamard's condition (c), also known as stability condition (or ill-conditioning), is intrinsic to inverse problems. It means that the EIT problem, which violates this condition, becomes extremely sensitive to the presence of errors, including experimental errors in the data and the numeric truncation errors in the computational procedure. The effect of well-conditioning direct problem (4) and ill-conditioning inverse problem (5) are sketched in the following figure. About this specific topic, some researchers have worked to develop regularization strategies for the EIT problem, aiming to reduce such extreme sensitivity.

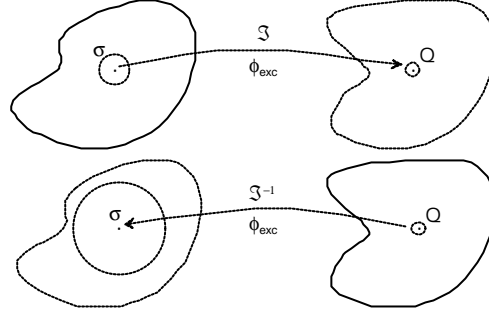


Figure 1 – schematic illustration of the influence of experimental errors and noise in the direct (Eq. (4) ) and inverse (Eq. (5) ) problems.

### 3. Solution of the inverse problem

Generally, the inverse problem represented by equation (5) is solved by devising an error functional that assesses the difference between the actual and the model electrical contrast distribution (conductance or permittivity) by comparing boundary measurements (electrical current or charge distribution) with the corresponding predictions from the model. The solution is constructed by refining the model contrast through an optimization heuristics, which is iterated until a good match is achieved between the actual measurements and the corresponding predicted values.

Let  $\sigma_{\text{actual}}$  be the actual electrical contrast, associated with the phase distribution of the flow inside the sensing volume, and let  $\sigma_{\text{approx}}$  be an approximated version of the actual contrast, which can be initially defined from the qualitative images delivered by a direct imaging probe (Seleglim and Hervieu, 1998). Considering a common excitation profile  $\phi_{\text{exc}}$ , the actual (measured) and the approximated (prospective) response profiles can be formally calculated with the help of definition (4) as the following:

$$Q_{\text{actual}} = \mathfrak{S}[\phi_{\text{exc}}, \sigma_{\text{actual}}] \quad (6)$$

$$Q_{\text{approx}} = \mathfrak{S}[\phi_{\text{exc}}, \sigma_{\text{approx}}] \quad (7)$$

in which  $Q_{\text{actual}}$  is measured directly from the experiment and  $Q_{\text{approx}}$  is determined numerically by solving equation (1) with adapted boundary condition from (2) such as

$$\phi(\xi, \eta) = \phi_{\text{exc}} \quad \text{for } (\xi, \eta) \in \partial\Omega \quad (8)$$

It should be clear that, in principle, what  $Q_{\text{approx}}$  and  $Q_{\text{actual}}$  have in common is only the excitation profile.

The difference between  $\sigma_{\text{actual}}$  and  $\sigma_{\text{approx}}$  (as seen according to a particular perspective defined by  $\phi_{\text{exc}}$ ) can be quantified by the functional (Euclidian norm)

$$e = \left\| Q_{\text{actual}} - Q_{\text{approx}} \right\| \quad (9)$$

A solution for the EIT problem can be constructed by minimizing the functional (9), i.e. by imposing that  $\delta e = 0$ , or through a parametrization of  $\sigma_{\text{approx}}$ , which transforms (9) into a function of such parameters, and subsequent search for the minimum through an adequate algorithm. The first alternative corresponds to a variational approach of the EIT problem and would lead to intricate nonlinear Euler-Lagrange type differential equations (Borcea, 2002). The second alternative corresponds to a functional approach of the EIT problem which inversion requires the solution of an optimization problem that also has complexities to be overcome. Independently of the approach adopted to reconstruct the electrical contrast distribution of the flowing multiphase mixture, such difficulties are intrinsic for the problem that is ill-posed and, probably, unsolvable in practice without regularization strategies.

### 4. Regularization strategies

The stability of a given EIT problem is influenced by its formulation. In other words, equivalent formulations of the same problem may result in completely different numerical properties and behavior; some may be regularizable while others may be totally unstable. In broad terms, a regularization method consists in determining an approximate smooth solution, compatible with the measured data and noise or error levels. Aligned with these ideas, a modified regularizable version of equation (9) is proposed:

$$e = \left\| Q_{\text{actual}} - Q_{\text{aprox}} \right\| + \alpha \left\| g[\sigma] \right\| \quad (10)$$

in which  $\alpha$  is the regularization parameter and  $g[\sigma]$  is the regularization operator. Minimizing (10) instead of (9) method corresponds to enforce simultaneously a good match between measured and modeled data, and that the solution must be smooth. The role of the regularization parameter is of balancing such requirements in the sense of giving more or less emphasis in smoothness as  $\alpha$  varies respectively from high values to zero.

Tikhonov's regularization (Tikhonov and Arsenin, 1977) is known as one of the most widely applied method for solving ill-posed problems. According with his original proposition, the regularization operator is defined as

$$g[\sigma] = \sum_{k=0}^P \mu_k \left\| \sigma^{(k)} \right\|^2 \quad (11)$$

where  $\sigma^{(k)}$  denotes the  $k$ th derivative of the contrast  $\sigma$  and  $\mu_k$  is a constant greater than zero, usually set as the Kronecker's delta:

$$\mu_k = \delta_{k,j} \quad (12)$$

in which case the operator (11) simplifies to

$$g[\sigma] = \left\| \sigma^{(j)} \right\|^2 \quad (13)$$

and the whole technique is called Tikhonov's  $j$ -order regularization. The most used regularization order is Tikhonov-0, which effect is to attenuate oscillations and, thus, producing a smoother reconstructed contrast. Despite the number of successful applications, Tikhonov's regularization technique suffers from the problem of identifying an adequate value for the regularization parameter ( $\alpha$  in (10)). In the case of multiphase flows, one can be interested in large structures (slug flow for instance), in which case high  $\alpha$  values should be used to improve the smoothing effect. Or, on the contrary, if one is interested in detailed structures (like small bubbles in bubbly flow), then small  $\alpha$  values should be used to increase the importance of the matching between the actual and the model measurements.

#### 4. Case study – Construction of error surfaces

Let us consider the EIT problem the flow of water in a square section tube with a small cubic air inclusion placed as indicated in the following figure:

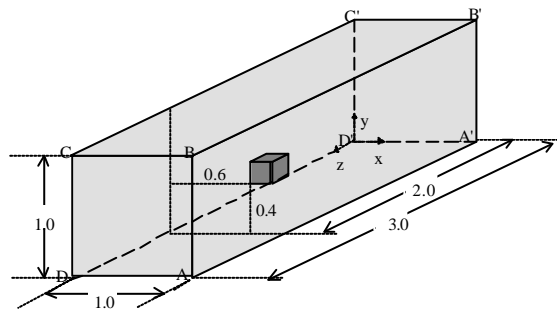


Figure 2 – Schematic representation of the sensing volume (the parallelepiped) with a small cubic bubble placed as indicated, which is simulated with the help of equations (1), (2) and (3)

A discrete version of the governing differential equation can be derived from a central difference scheme, noting that is not necessary to apply (1) at the boundaries because these values are known from the imposition of the excitation profile  $\phi_{\text{exc}}$ . In particular, boundary conditions were adopted aiming to simulate three different excitation profiles: classical Dirac, pyramidal and ridge-Dirac. Previous experimental and numerical results have shown that the form of the excitation profile has a profound effect on the topology of the error surface (Rolnik and Selegim, 2001). In the case of classical Dirac excitation, widely applied but with an intrinsic lack of sensitivity (Figueroa and Selegim, 2001), consists in exciting through a point electrode and grounding of the remaining of the boundary. An alternative to this is the pyramidal excitation strategy, which can be generated by varying the potential from its maximum value, at the center of the upper boundary surface, to a minimum value occurring on the median segment of the opposed side. This excitation profile has the advantage of inducing the electrical sensing field to cross the measurement volume. Since the

pyramidal distribution presents some practical difficulties to be put into practice, the ridge-Dirac represents an interesting trade-off between these two, following approximately the idea mentioned above, and easily generated by a segment excitation placed long the upper median segment. In mathematical terms these excitation profiles represent new Dirichlet-type boundary conditions according with (2), and will be introduced in the simulations directly into the discretized version of the governing equation (1). The following figure shows the four longitudinal faces on which such boundary conditions were applied. Neumann-type boundary conditions were imposed on the transversal sides (ABCD and A'B'C'D' in figure 2) in order to prevent the sensing volume becoming infinite.

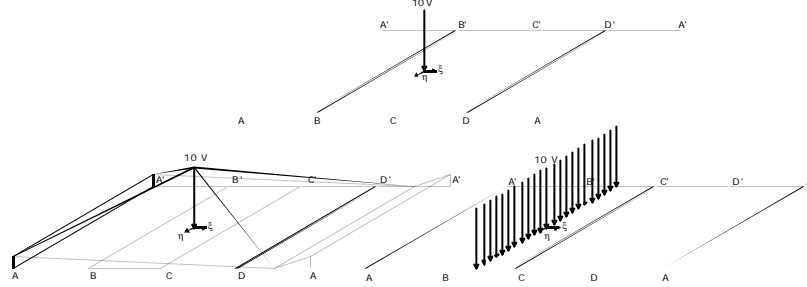


Figure 3 – Different excitation profiles / boundary conditions for the governing equation (1): (top) Dirac, (down left) pyramidal and (down right) ridge-Dirac.

The computational domain is composed of  $21 \times 21 \times 61$  nodal points regularly spaced ( $\Delta = 0.05$ ) respectively in x, y and z directions. The electrical contrast  $\sigma$  was defined in order to represent the continuous phase with a small three-dimensional cubic inclusion with sides equal to one mesh step, as indicated in figure 2. Numerical values were attributed to  $\sigma$  to reproduce the flow of water ( $\sigma_{\text{actual}} = 80$ ) in air ( $\sigma_{\text{actual}} = 1$ ).

The visualization of the error surfaces can be obtained through different contrast model distributions, generated from some convenient systematic changes in the contrast  $\sigma$ . For instance, a prospective  $\sigma$  was generated by translating the inclusion along a horizontal and a vertical planes passing through its original position and the corresponding two-dimensional error surfaces were computed. This study (Rolnik and Selegim, 2001) revealed some important characteristics, called pathologies, such as extremely pronounced minimum (the solution well), saddle points, boundary minima and flat regions. Another similar study revealed an even more problematic situation in which the solution minimum is surrounded by ring maxima, which may seriously compromise the effectiveness of numerical minimization methods (Campos et al, 2002). In this paper error surfaces are constructed by varying the contrast values between fixed known limits and assuming that format, dimensions and location of the inclusion are known. It will be shown that important pathological features of the corresponding error surfaces are revealed.

Let then  $\sigma_{\text{int}}$  and  $\sigma_{\text{ext}}$  denote the contrast value in the interior and exterior region of the cubic inclusion respectively. Also, let  $Q_{\text{approx}} |_{\sigma_{\text{int}}, \sigma_{\text{ext}}}$  indicate the corresponding response profile obtained with the help of the excitation profiles as defined above, that is

$$Q_{\text{approx}} |_{\sigma_{\text{int}}, \sigma_{\text{ext}}} = \mathfrak{F} \left[ \phi_{\text{exc}}, \sigma_{\text{approx}} |_{\sigma_{\text{int}}, \sigma_{\text{ext}}} \right] \quad (14)$$

It is then possible to calculate the error between  $Q_{\text{approx}} |_{\sigma_{\text{int}}, \sigma_{\text{ext}}}$  and the correct measured profile  $Q_{\text{actual}}$  for a number of combinations of  $\sigma_{\text{int}}$  and  $\sigma_{\text{ext}}$  in limited intervals, through an adaptation of definition (9) according with the following:

$$e_{\text{approx}} |_{\sigma_{\text{int}}, \sigma_{\text{ext}}} = \left\| Q_{\text{approx}} |_{\sigma_{\text{int}}, \sigma_{\text{ext}}} - Q_{\text{actual}} \right\| \quad (15)$$

The following figure shows the error surfaces obtained by plotting (15) with respect to  $\sigma_{\text{int}}$  within  $[0.2, 2.2]$  and  $\sigma_{\text{ext}}$  varying within  $[50, 100]$ , and for the Dirac, pyramidal and ridge-Dirac excitation profiles. The adopted segmentation of these intervals implies in calculating 121 times the error function, which took 30 minutes in a 1.5 GHz PC. The global minimum attraction domain (solution well) can be identified in all three plots, embedded in its characteristic pathological geometric feature corresponding to the long and narrow valley. Convergence of a numerical minimization procedure can be extremely complicated in this condition. For instance, an algorithm based on the local inclination, after falling inside the valley will progress only if very small correction steps are taken because of the intrinsic imprecision in determining the steepest inclination. In other words, any iteration step in a slightly incorrect direction will toss the minimization sequence out of the valley, resulting in huge and possibly unstable oscillations, or in

a premature convergence. Convergence is equally problematic for minimization methods based on evolutionary heuristics. Once the minimization sequence is inside the valley all strong mutations will produce descendants outside the valley and consequently tending to be discarded. The only way that convergence is assured is by allowing delicate mutation to be performed, which results in small correction steps and significant increase in the total number of generations needed to reach the solution.

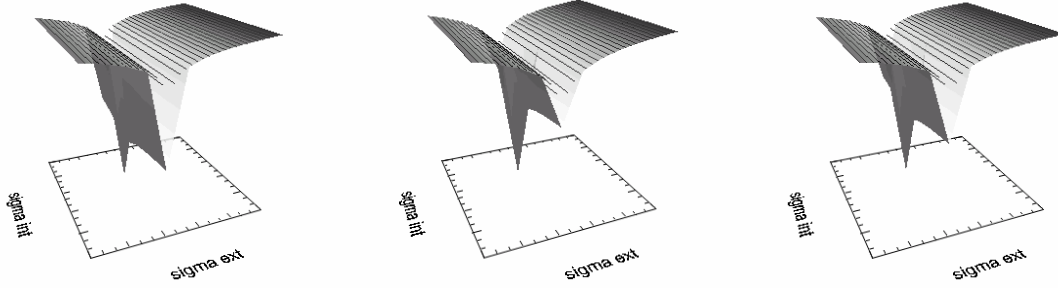


Figure 4 – Error surfaces (equation (15)) for  $\sigma_{int}$  within [ 0.2 , 2.2 ] and  $\sigma_{ext}$  within [ 50 , 100 ], and for the Dirac (left), pyramidal (center) and ridge-Dirac (right) excitation profiles

Although the pathology of all the error surfaces in figure 4 is the same, its severity is affected by the excitation profile. The worst case corresponds to the classical Dirac excitation (the associated valley is the most sharp and deep), which confirms that this technique has an intrinsic lack of sensitivity (Figueroa and Selegim, 2001). Pyramidal and ridge-Dirac excitation produces slightly better optimization surfaces, although the valley is still present suggesting that a regularization procedure is needed to palliate the problem. In this work we adopted the following regularization operator for equation (10):

$$g[\sigma] = \begin{cases} \left| \|\sigma_{num}\| - V_F \right|^{-1} & \text{if } \|\sigma_{num}\| \neq V_F \\ \Delta & \text{if } \|\sigma_{num}\| = V_F \end{cases} \quad (16)$$

in which  $V_F$  stands for the measured void fraction of the flow and  $\Delta$  is a positive constant conveniently defined. The influence of this particular regularization operator can be inferred from the following figure in which (16) is plotted for  $\sigma_{int}$  and  $\sigma_{ext}$  varying in the proper intervals (same as in figure 4). It is possible to observe in figure 5 that the region of the solution well is preserved while the valley is transformed into a crest. Consequently, the introduction of (16) into (10) with the proper regularization parameter  $\alpha$  will cancel out most of the negative topological features of the error surface.

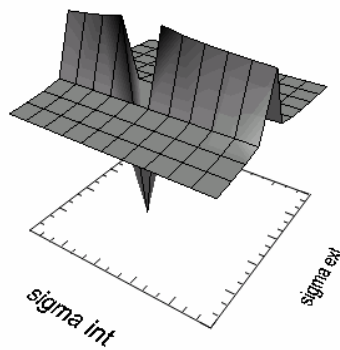


Figure 5 – Plot of the regularization operator (equation (16)) for  $\sigma_{int}$  within [ 0.2 , 2.2 ] and  $\sigma_{ext}$  within [ 50 , 100 ]

Determining the best  $\alpha$  is still an open problem, mainly because there is no comprehensive theoretical framework assessing the relation among the severity of the ill-posedness of the problem, the specific formulation of the regularizing operator and the associated regularizing parameter. In simpler terms, determining the best  $\alpha$  is usually done through a trial-and-error procedure. In this work the best  $\alpha$  was defined to be the one for which the pathology of the error surface is less severe, that is, for which the valley containing the solution well becomes broader and less deep. The following figure shows the best cases for each excitation profile considered. It is possible to assume that the possibilities of attaining convergence has been greatly enhanced, despite some negative topological feature still remains as, for instance, the negative inclination at the bottom of the valley. In this regard, an optimization method based on the local

inclination will suffer because of this remaining negative feature while it is probably almost indifferent for an evolutionary based method.

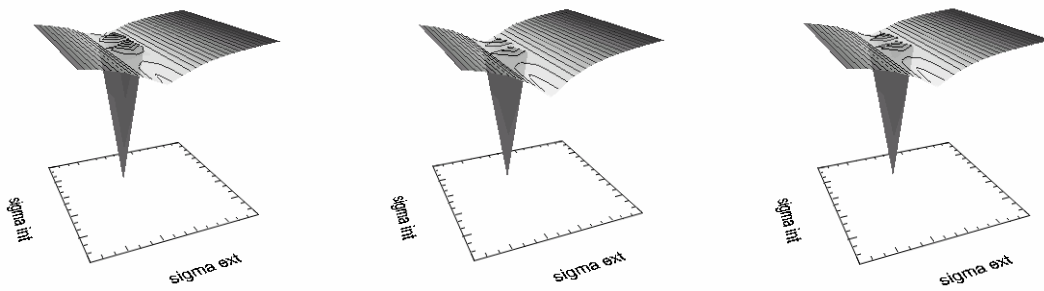


Figure 6 – Plot of the regularized optimization surfaces for Dirac (left) pyramidal (center) and ridge-Dirac (right) excitation strategies ( $\sigma_{int}$  within [ 0.2 , 2.2 ] and  $\sigma_{ext}$  within [ 50 , 100 ]).

#### 4. Conclusions and perspectives

Inverse EIT problems are intrinsically ill-posed. According to the formulation of the problem adopted in this work (minimization of an error functional), this mathematical fact is associated with the number of negative topological features of the optimization surface (pathology), which prevents most of the minimization sequences from converging to the global minimum. Regularizations schemes are commonly used to stabilize the numerical procedure, especially in the presence of experimental measurement noise and computational truncation errors. The most widely used regularization method falls into the so-called Tikhonov's strategy, although we adopted a somewhat different approach in this work. More specifically, preliminary tests of a different regularization operator were performed, aiming to contribute in the development of a new reconstruction algorithm for the EIT problem. The proposed regularization operator (16) consists in comparing the model and the measured void fraction of the flowing multiphase mixture, which can be obtained respectively by a weighted integration of the model contrast distribution and by a proper processing of the response signals delivered by the imaging probe. Numerical experiments were performed considering the flow of water in a square section tube with a small cubic air inclusion, and comparing different excitation strategies (Dirac, pyramidal and ridge-Dirac). In order to define a two-dimensional optimization surface to facilitate visual analysis, we considered the position and form of the inclusion as already known and varied the electrical contrast of the continuous and dispersed phase within representative limits. Results show that, although the excitation strategy has a strong influence on the original problem, the proposed operator was capable of minimizing the pathology of the problem in all cases, after proper adjustment of the regularization parameter ( $\alpha$  in (10)).

#### 5. Acknowledgement

The authors would like to acknowledge the financial support provided by FAPESP thought grants 99/02821-2 and 02/13343-9.

#### 6. References

- Borcea, L.,2002, "Electrical Impedance Tomography", *Inverse Problems*, Vol. 18, pp. R99-R136.
- Campos, G.P., Rolnik, V.P. and Seleglim Jr, P.,2002, "Patologias dos problemas inversos de reconstrução térmica – desenvolvimento d e uma técnica de reconstrução tridimensional", *Proceedings of the II Congresso Nacional de Engenharia Mecânica (CONEM2002)*, João Pessoa – PB, Brazil.
- Figuroa, T. P. and Seleglim Jr. P.,2001, "Sensitivity Analysis of Different Sensing Strategies for Electrical Impedance Imaging of Two-Phase Flows", *Journal of Electronic Imaging*,Vol. 10(3), pp. 641-645.
- Hadamard, J.,1902, "Sur les problemes aux dérivées partielles et leur signification physique", *Bull. Univ. Princeton*, 13, p.49-52.
- Lányi, S.,1998, "Analysis of linearity errors of inverse capacitance position sensors", *Meas. Sci. Technol.*, Vol. 9, pp.1757-1764
- Nachman, A.I., 1988, "Reconstructions from boundary measurements", *Annals of Mathematics*, Vol. 128, pp.531-576.
- Rolnik, V.P. and Seleglim Jr.,P.,2001. "Contribution to the Development of a New Image Reconstruction Method for Two-Phase Flow Electrical Impedance Tomography – Topological Studies", *Proceedings of the 2nd International Conference on Computational Heat and Mass Transfer*, Rio de Janeiro, Brazil.
- Seleglim Jr., P.; Hervieu, E.,1998, "Direct imaging of horizontal gas-liquid flows", *Meas. Sci. Technol.*, Vol. 9, No.8, pp. 1492-1500.
- Seleglim Jr., P. and Milioli F.E.,2001. "Improving the determination of bubble size histograms by employing wavelet de-noising techniques". *Powder Technology*, Vol. 115, pp.114-123.
- Tikhonov, A. N. & Arsenin, V.Y., 1977, *Solution of Ill-posed Problems*, John Wiley & Sons.